

Elastic Scattering and Polarization of Protons by Helium at 147 and 66 Mev

A. M. CORMACK,* J. N. PALMIERI, N. F. RAMSEY, AND RICHARD WILSON
Cyclotron Laboratory, Harvard University, Cambridge, Massachusetts

(Received March 2, 1959)

Measurements have been made of the polarization and differential cross section in elastic $p\text{-}\alpha$ scattering at 147 and 66 Mev, in the laboratory angular ranges of $2^\circ\text{--}165^\circ$ and $10^\circ\text{--}45^\circ$, respectively. These have been compared with recent calculations which relate the scattering amplitudes to nucleon-nucleon results. Because these calculations take into account the angular variation of the nucleon-nucleon amplitudes, better agreement is obtained than heretofore. A comparison of the polarization with that observed in inelastic scattering from several levels of a variety of spin-zero nuclei indicates a strong similarity between the elastic and inelastic data, which can be explained theoretically.

I. INTRODUCTION

THE perennial study of the elastic scattering of protons by nuclei has been stimulated in the last few years by the introduction of polarization measurements, which provide additional information about scattering processes. Further stimuli have been provided by attempts^{1,2} to relate the scattering and polarization from complex nuclei to the rapidly accumulating information about polarization in nucleon-nucleon scattering. In these studies, light nuclei play an important role because of the relative unimportance of the form-factor and multiple scattering, which are dominant in heavy nuclei. Of the light nuclei, those with zero spin are the simplest to analyze, and, therefore, helium is worthy of particularly close study. Helium is also important from a purely experimental point of view. The experimental study of polarization phenomena requires good analyzers, and helium, because of the high polarizations produced at certain angles, is useful in this capacity, despite the awkwardness of handling it in the liquid form.

High-energy experiments have been done on the scattering of protons by helium,³⁻⁶ but, with the exception of reference 6, these either cover a rather small angular range or else lack any information about polarization. In addition, no data are available near 150 Mev, the energy of the Harvard synchrocyclotron. It therefore seemed desirable to use the apparatus, which had been made in this laboratory for the study of proton-proton scattering, to measure the scattering from helium. The target could be used equally well for liquid hydrogen or liquid helium. The counter telescopes had sufficient energy resolution to separate

protons scattered elastically from helium from those scattered inelastically, over a wide range of angles. Since this apparatus has been described in detail elsewhere (by Palmieri *et al.*,⁷ hereafter referred to as I), only a brief description of it will be given here.

Measurements have been made of the differential cross section and polarization from 2° to 165° lab at the full energy of the cyclotron. In addition, some measurements were made at 66 Mev. Because of the finite size of the target and consequent large energy loss of low-energy particles in traversing it, these only covered the limited angular range of 10° to 45° lab.

II. EXPERIMENTAL METHOD

Measurements were made by scattering the polarized proton beam off a liquid helium target, which was situated outside the shielding of the cyclotron, and by detecting the scattered protons with a counter telescope. Data were accumulated in six different runs, details of which are given in Table I. At various times two telescopes and four experimental arrangements were used, the latter being shown schematically in Fig. 1.

The Polarized Proton Beam

The polarized proton beam is obtained by scattering the internal beam of the cyclotron off carbon at about

TABLE I. Pertinent information on the accumulation and treatment of the data in the various runs. I.C. and F.C. refer to the ionization chamber and Faraday cup, respectively. See Fig. 1 for diagrams of the "experimental arrangements."

Run	Experimental arrangement	East probe	Laboratory angular range	Normalization	Monitor
1a	A	In	$6^\circ\text{--}17.5^\circ$	Carbon	I.C.
1b	A	Out	15° and 20°	Carbon	I.C.
2a	A	Out	$15^\circ\text{--}90^\circ$	Carbon	I.C.
2b	D	Out	$90^\circ\text{--}120^\circ$	90°, Runs 1 and 2a	I.C.
3	B	Out	$90^\circ\text{--}165^\circ$	90°, Runs 1 and 2a	I.C.
4a	A	In	15° and 20°	Carbon	F.C.
4b ^a	A	In	$10^\circ\text{--}45^\circ$	Carbon	F.C.
5	C	In	$3^\circ\text{--}10^\circ$	Run 1	I.C.
6	C	In	$2^\circ\text{--}7^\circ$	Run 1	I.C.

^a Run 4b was the only run made at 66 Mev.

⁷ Palmieri, Cormack, Ramsey, and Wilson, *Ann. Phys.* **5**, 299 (1958).

* On leave from the University of Cape Town, South Africa. Now at Tufts University, Medford, Massachusetts.

¹ H. A. Bethe, *Ann. Phys.* **3**, 190 (1958).

² H. McManus and R. M. Thaler, *Phys. Rev.* **110**, 590 (1958).

³ Chamberlain, Segrè, Tripp, Wiegand, and Ypsilantis, *Phys. Rev.* **102**, 1659 (1956).

⁴ M. K. Brussel and J. H. Williams, *Phys. Rev.* **106**, 286 (1957).

⁵ Kruse, Selove, and Teem (private communication); see W. Selove and J. M. Teem, *Phys. Rev.* **112**, 1658 (1958).

⁶ K. Gotow (private communication). *Note added in proof.*—These results are now compiled in a report (NYO-2532) of the Department of Physics and Astronomy of the University of Rochester (unpublished).

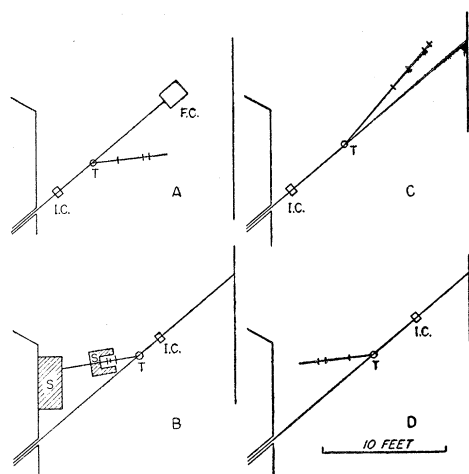


FIG. 1. Schematic diagrams of the experimental arrangements used in the various runs. See Table I for details. I.C.—ionization chamber; F.C.—faraday cup; T—target; S—additional shielding.

17° . The nature of the beam may be varied by changing the position of a brass block which may intercept the internal beam. This is known as the "east probe." A full description of the method of extraction of the beam and of the effect of the east probe (on the beam) has been given by Calame *et al.*⁸ Regenerated orbits of low-energy components of the internal beam fall outside the orbits of higher-energy protons. If the east probe is out, both the high- and low-energy components of the beam emerge from the tank, but if the probe is moved in, the low-energy components are stopped by the probe, and the result is an external beam of lower intensity but smaller energy spread than if the probe were out. In these experiments two positions of the east probe were used, and these will be designated by "east probe in" and "east probe out." With the east probe in, the beam had an intensity of 3×10^6 protons per second through a $\frac{3}{8}$ -in. \times $1\frac{1}{2}$ -in. slit, its energy was 147 Mev with a full width of 2 Mev, and the polarization was $72 \pm 2\%$. With the east probe out, the beam had an intensity of 10^7 protons per second through a $\frac{3}{4}$ -in. \times $1\frac{1}{4}$ -in. slit, its energy was 145 Mev with a full width of nearly 4 Mev, and the polarization was $62 \pm 2\%$. The higher-intensity beam was normally used for the larger angles where the cross sections are smaller, and the lower-intensity beam was used for the smaller angles. For runs 4b, 5, and 6, the defining slit was reduced in size to $\frac{1}{2}$ in. \times 1 in. and the flux through it was 5×10^5 protons per second. In order to obtain results at 66 Mev, it was necessary to reduce the energy of the beam. This was done by placing absorbers in the beam. Liquid hydrogen was used to reduce the energy to 72 Mev, and the remainder of the slowing down was done with polyethylene. The figures given

⁸ Calame, Cooper, Engelsberg, Gerstein, Koehler, Kuckes, Meadows, Strauch, and Wilson, *Nuclear Instr.* **1**, 169 (1957).

above for the energies of the beam are the energies at the center of the full target.

Since the angle of scattering off the carbon in the cyclotron tank was not known accurately, the beam polarizations were determined by scattering externally off carbon at 15° and measuring the asymmetries in the manner described below for the measurement of the helium asymmetries. The asymmetries thus found were then compared in the Born approximation with the Harwell 135-Mev⁹ and Uppsala 155-Mev¹⁰ results for carbon, and the beam polarizations were inferred.

The Target

A complete description of the target is given in I. The essential part was a cylinder of two-mil Mylar, two inches in diameter and three inches high, which contained the liquid helium used as the target material. The Mylar was silvered to prevent loss of helium by radiation, and this silvering possibly also reduced loss of helium by diffusion through the Mylar into the surrounding vacuum. The Mylar target was surrounded by a heat shield which introduced $\frac{1}{2}$ mil of aluminum foil into the beam; the vacuum was contained in a system which introduced two Mylar windows into the direct beam. These were made of three-mil Mylar, but the only one which could be seen by the counter telescope was wrinkled rather irregularly so that its effective thickness was possibly 50% higher. The Mylar target was attached to a two-liter reservoir which, when filled, kept the target full for six to eight hours.

The Counter Telescopes

Two of these were used, and they are fully described in I. The small-angle telescope consisted of four plastic scintillation counters in coincidence, the defining counter being ten feet from the target, $1\frac{3}{4}$ in. wide, and $4\frac{1}{2}$ in. high, giving an angular resolution of 1° lab. This was only used in the angular range of 2° to 10° lab. and is shown schematically in Fig. 1 as arrangement C. The large-angle telescope consisted of three of the above-mentioned plastic scintillation counters in coincidence, with the same defining counter. In runs 1, 2, and 4, the defining counter was four feet from the target, giving an angular resolution of $2\frac{1}{2}^\circ$ lab. In run 3 the defining counter was two feet from the target, and the angular resolution was 5° . The angular resolutions given above are full widths at half height and include the effects of the angular divergence of the beam and the finite size of the target.

Helium has no excited states, but protons may be inelastically scattered with an energy less than the energy of elastically scattered protons by 20 Mev or more in the center-of-mass system; these must be excluded by the counter telescope. This exclusion was

⁹ A. E. Taylor (private communication).

¹⁰ Alphonse, Johansson, and Tibell, *Nuclear Phys.* **4**, 672 (1957).

accomplished by inserting absorber between the last two counters of the telescope so that elastically scattered protons could reach the last counter, but inelastically scattered protons could not. The absorbers used were copper in runs 5 and 6, and otherwise polyethylene. This technique easily separated the inelastics from the elastics at small angles where only the 2-Mev spread in beam energy smeared the difference in energy between the two groups, but the separation became progressively more difficult with increasing angle. At scattering angles near 165° , the beam energy had a spread of 4 Mev, and, in addition, some elastically scattered protons traversed the target twice, losing energy in the process, while some inelastically scattered protons entered the target and were immediately scattered so that they lost no energy in the target. Taking these factors into account, calculations showed that at 165° the minimum energy of elastically scattered protons leaving the target was 41.6 Mev, while the maximum energy of the inelastically scattered protons was 39.1 Mev. The maximum energy of elastically scattered protons leaving the target was 52.7 Mev, and the energy required to reach the last counter without penetrating it was 42.0 Mev. Thus a few elastically scattered protons were not counted. This loss was estimated to be at most 5%, and the cross section at 165° may be low by this amount. The asymmetry could be affected by this loss of low-energy particles in two ways. First, there would be an obvious effect if the lost protons had a polarization substantially different from those counted, and second, even if they had the same polarization, there is a slight energy spread across the beam which might make the loss asymmetric between right and left. The effect of these is the same for the two cases, namely an asymmetry in the loss of protons. Since the measured polarization at 165° is zero, the greatest error that such an asymmetry could produce is of the order of the percentage of protons lost. Since this is at most 5% and since the quoted error in the polarization at 165° is 0.15, these considerations do not affect the quoted result materially.

For run 4b (66 Mev) the factor which limited the angular range to 10° – 45° was not the separation of elastics from inelastics, but the energy loss in the target and counters. This was such that at angles greater than 45° the energy of some of the scattered particles was not sufficient for them to be able to traverse the target and reach the last counter. At the 45° angle, the maximum-energy inelastics and the minimum-energy elastics were separated by 8 Mev, so that the inelastics were easily excluded.

Monitoring

An argon-filled ionization chamber was used to measure the beam after the defining slit in all runs; in addition, in runs 2a and 4, a Faraday cup was used to collect the beam. While the Faraday cup and the

ionization chamber agreed well within each run, their ratio was different for the two runs. The Faraday cup was used (but not in an absolute sense) as a monitor in runs 2a and 4, and the ionization chamber in the rest.

Alignment

Great care was taken to determine the zero from which the scattering angles were measured. The counters were aligned optically, with respect to each other, on the arm which supported them, and the pivot of this arm was located under the target. After the zero angle had been found roughly by photographic methods, the telescope was swept through the beam in small steps. At each step the integrated anode current of the phototube attached to the defining crystal was measured. From the symmetrical curve so obtained, it was possible to determine the zero-angle position to within 0.02° for runs 1 to 4, and within 0.005° for runs 5 and 6.

Backgrounds

At angles of 15° to 100° the backgrounds were of the order of 5% to 10% of the counting rate from helium alone. They increased in the forward direction, becoming 35% at 2° . To ensure that background particles entered the last crystal of the counter telescope with the same energy when they were measured as when the data on helium were being taken, extra absorber was placed in the counter telescope in the measurement of some of the small-angle backgrounds. This absorber was chosen to compensate for the thickness of helium. The presence of this absorber produced no change of a magnitude to affect the results. At small angles a helium-filled bag was placed in the direct beam, immediately after the target. This produced a background lower than that due to the air which would have occupied the same volume.

At angles greater than 100° , the backgrounds became progressively more serious until at 160° they equalled the rate from helium itself; at 165° they exceeded it by a factor of $2\frac{1}{2}$. At the large angles the backgrounds were measured in two ways: one with the normal amount of absorber in the telescope, the other with additional absorber which had the same effect on the energy of the scattered protons as traversing the helium target twice. This was done because a substantial part of the background was due to scattering from the Mylar walls of the helium target and from the window of the vacuum chamber. About one quarter of this part of the background came from the wall away from the counter telescope, and so was affected by the presence of helium. To take this into account, the background was calculated by averaging the measured values with and without the extra absorber in the telescope in the ratio 1:3. The uncertainty in the cross section arising from this procedure is estimated as 15% to 165° and 8% at 160° .

Another source of the backgrounds at 160° and 165° was neutrons from the cyclotron itself. These produced proton recoils in or near the last counter, and the protons traversed the counter telescope backwards. This effect was reduced by lead and steel shielding several feet thick as shown in Fig. 1B.

Measurement of Polarization and Cross Section

If an unpolarized beam strikes a target and is scattered at an angle θ_1 , the scattered beam will have a polarization $P_1(\theta_1)$, where P_1 is characteristic of the target and is the expectation value of the spin in a direction normal to the plane of scattering. If this scattered beam strikes a second target, the amounts of scattering to the left and right at an angle θ_2 will not in general be the same. If σ_R and σ_L are the differential cross sections for scattering to the left and right, respectively, then the asymmetry $e(\theta_2)$ is defined as

$$e = (\sigma_R - \sigma_L) / (\sigma_R + \sigma_L).$$

Wolfenstein¹¹ shows that $e = P_1(\theta_1)P_2(\theta_2)$, where $P_2(\theta_2)$ is the polarization which would be produced if an unpolarized beam were scattered by the second target at the angle θ_2 . Also, if σ is the cross section of the second target for an unpolarized beam, then¹¹

$$\sigma_R = \sigma(1 + P_1P_2),$$

$$\sigma_L = \sigma(1 - P_1P_2).$$

Thus measurements of the scattering to left and right at a given angle suffice for the determination of both the polarization and the unpolarized differential cross section.

In a typical run the order in which measurements were taken was as follows. The scattering from carbon at 15° was measured, if possible. Backgrounds for helium were taken. The helium asymmetries were measured, the measurements at each angle being made at least twice. The backgrounds were repeated, and the scattering from carbon was measured again. The two sets of backgrounds were reproducible within statistics, so no additional measurements were made during the run to check that they were constant. In runs where it was possible to take them, the carbon measurements served two purposes. First, they gave a measurement of the polarization of the proton beam, as described above, and, second, they provided data for the normalization of the relative cross sections, as described below.

Corrections

Corrections were made for the following effects: dead times of scalers, double scattering in the target, scattering and absorption in the counter telescope, the finite height of the counters which affected the polarization at small angles, and the dependence of the back-

grounds on the beam energy. The last correction must be made because about three quarters of the backgrounds at small angles came from material in the direct beam after the target. Protons which were scattered from this material thus had a lower energy when the target was full than they had when the backgrounds were measured. All these corrections are discussed in detail in I and were applied in the same way as in I, with obvious modifications for the differences in targets and scattering kinematics.

Normalization of Cross Sections

In runs 1, 2a, and 4, measurements were made of the scattering from carbon at 15° , in order to determine the polarization of the beam, and the helium data of these runs were normalized (relatively) to the carbon results. No significant differences were found between the data taken with the east probe out and with it in, so they were averaged to give relative cross sections in the range 6° to 90° lab. With experimental arrangements B, C, and D (see Fig. 1), it was not possible to measure the scattering from carbon. The large-angle data of run 3 were normalized to the above data at 90° . The small-angle data of runs 5 and 6 were also normalized to the cross sections of runs 1, 2a, and 4a, the normalization factor being the mean ratio of the relative cross sections at angles common to the runs. In the regions 6° to 8° and around 90° , the departure of the cross sections from a linear variation with angle within the angular range subtended by the counters was so small that no correction was made for the fact that the angular resolution was not the same in all runs.

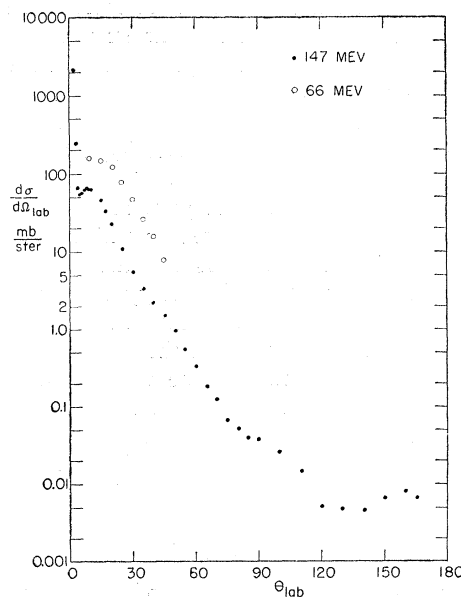


Fig. 2. Angular distribution of the p - α laboratory differential cross sections at 66 and 147 Mev. Because of the logarithmic scale, the errors would not be apparent except at the largest angles and have therefore been omitted.

¹¹ L. Wolfenstein, *Annual Review of Nuclear Science* (Annual Reviews, Inc., Palo Alto, 1956), Vol. 6, p. 43.

TABLE II. Final cross sections and polarizations averaged over all the runs. Cross sections are in mb/sterad.

θ_{lab}	$\theta_{\text{c.m.}}$	$\frac{d\sigma}{d\Omega}$ lab	$\frac{d\sigma}{d\Omega}$ c.m.	P
147 Mev				
1.96	2.46	2125±41	1345±26	-0.073±0.020
2.98	3.75	240.6 ±3.9	152.4 ±2.5	0.019±0.019
4.03	5.07	66.0 ±1.3	41.8 ±0.8	0.244±0.019
5.00	6.28	54.1 ±1.1	34.3 ±0.7	0.437±0.019
6.00	7.54	59.2 ±0.6	37.6 ±0.4	0.406±0.009
7	8.79	64.7 ±0.6	41.1 ±0.4	0.415±0.009
8	10.05	67.6 ±0.8	43.0 ±0.5	0.404±0.012
9	11.30	66.4 ±0.6	42.3 ±0.4	0.416±0.009
10	12.56	65.3 ±0.8	41.6 ±0.5	0.488±0.012
15	18.81	46.2 ±0.38	29.7 ±0.24	0.642±0.009
17.5	21.92	31.8 ±0.58	20.6 ±0.37	0.802±0.022
20	25.03	23.6 ±0.30	15.4 ±0.19	0.844±0.010
25	31.21	10.5 ±0.095	6.95 ±0.063	0.985±0.011
30	37.34	5.71 ±0.076	3.85 ±0.051	0.748±0.015
35	43.43	3.36 ±0.048	2.32 ±0.033	0.323±0.015
40	49.43	2.17 ±0.038	1.54 ±0.027	-0.123±0.023
45	55.37	1.54 ±0.029	1.12 ±0.021	-0.415±0.023
50	61.28	0.951 ±0.015	0.720 ±0.011	-0.684±0.020
55	66.99	0.532 ±0.012	0.414 ±0.009	-0.725±0.033
60	72.66	0.337 ±0.006	0.272 ±0.005	-0.856±0.025
65	78.23	0.183 ±0.0038	0.153 ±0.0032	-0.988±0.033
70	83.70	0.118 ±0.0029	0.103 ±0.0025	-0.869±0.025
75	89.08	0.068 ±0.0019	0.062 ±0.0017	-0.589±0.049
80	94.30	0.052 ±0.0010	0.049 ±0.0009	-0.500±0.030
85	99.45	0.040 ±0.0009	0.040 ±0.0009	-0.241±0.045
90	104.48	0.039 ±0.0010	0.039 ±0.0010	0.206±0.028
100	114.20	0.026 ±0.0014	0.030 ±0.0016	0.219±0.075
110	123.48	0.014 ±0.0009	0.017 ±0.0011	0.107±0.108
120	132.38	0.0051±0.0004	0.0069±0.0005	-0.07 ±0.15
130	140.09	0.0049±0.0003	0.0071±0.00043	-0.34 ±0.09
140	149.12	0.0045±0.0003	0.0069±0.00044	-0.35 ±0.09
150	157.02	0.0067±0.0003	0.0110±0.00054	-0.09 ±0.06
160	164.83	0.0082±0.0008	0.0139±0.0014	-0.07 ±0.07
165	168.65	0.0069±0.0014	0.0119±0.0024	0.00 ±0.15
66 Mev				
10	12.52	159.4±1.7	102.2±1.1	0.112±0.007
15	18.76	154.6±1.1	100.0±0.7	0.117±0.006
20	24.97	119.0±0.8	77.9±0.5	0.111±0.006
25	31.14	79.0±0.5	52.5±0.4	0.142±0.008
30	37.26	48.1±0.34	32.6±0.23	0.129±0.008
35	43.33	27.8±0.28	19.2±0.19	0.100±0.013
40	49.34	15.2±0.26	10.8±0.18	0.083±0.023
45	55.27	7.9±0.19	5.8±0.14	-0.014±0.035

In order to establish the absolute scale for the cross sections, the results of I were used. In I the scattering from carbon was measured under circumstances

identical to those of the present work, so it could be related directly to the absolute scale established for the proton-proton scattering. The error in the absolute cross section is 5%, as in I.

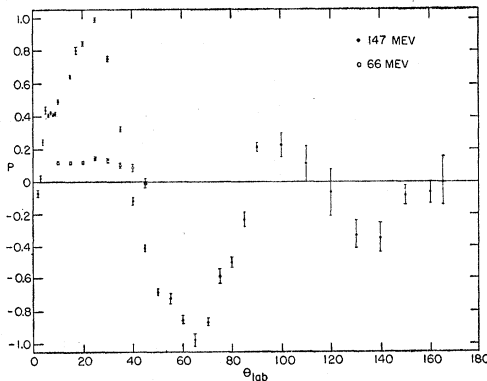


FIG. 3. Angular distribution of the polarization in the laboratory system in p - α scattering at 66 and 147 Mev.

III. RESULTS

The results are listed in Table II, where the errors given do not include the error in the absolute scale. Data are plotted in Figs. 2 and 3, which show the laboratory cross section and polarization as functions of laboratory angle. The angular resolution in the laboratory system is 1° , 2.5° , and 5° in the ranges $2^\circ \leq \theta \leq 10^\circ$, $15^\circ \leq \theta \leq 120^\circ$, and $\theta > 120^\circ$, respectively.

Comparison with the work of other laboratories is made in Figs. 4 and 5. In these, the laboratory cross sections and polarizations have been plotted against the momentum transfer $q = 2k \sin(\theta/2)$, in order to take energy differences into account. It must be pointed out that the 93-Mev results of Kruse, Selove,

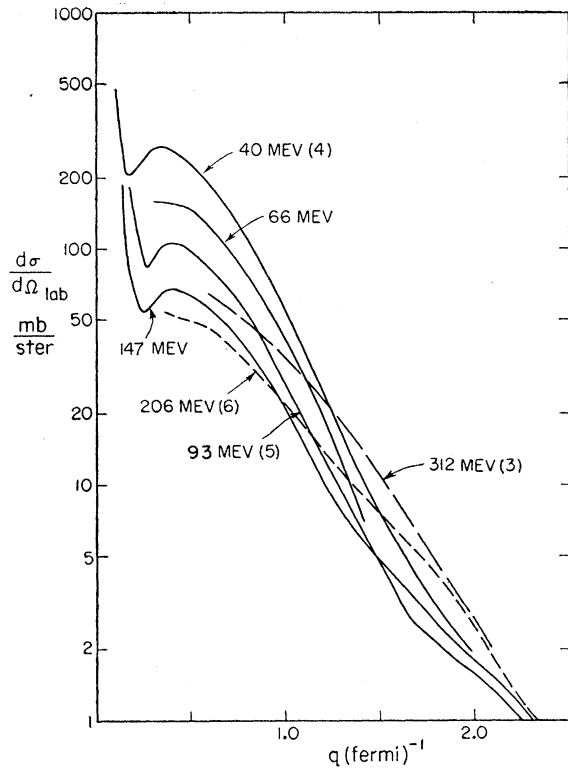


FIG. 4. p - α laboratory differential cross section at several energies. The energy differences are accounted for by plotting the cross section against $q=2k \sin(\theta/2)$. Smooth curves have been drawn through the experimental points. Numbers in parentheses are the references to the experimental data. The 93- and 206-Mev results are not corrected for absorption losses in the counter telescopes.

and Teem,⁵ and the 93-Mev and 206-Mev results of Gotow⁶ are not their final results, and absorber corrections have still to be applied, which might be about 15% at small angles and which will drop to zero at large angles. The cross sections will thus be increased when this correction is made, but presumably Gotow's polarization measurements should not be appreciably changed. k is the laboratory momentum.

The principal features of the cross-section variations are as follows. (a) From 40 Mev to 147 Mev, the Coulomb interference dip has about the same size, while at 206 Mev it seems to have almost disappeared. Unfortunately the range of q for the 312-Mev data does not extend to small enough values to give information on this point; the disappearance of the Coulomb interference dip is to be expected, however, from data on carbon and shows a vanishing of the real part of the scattering amplitude. (b) For $q=0.5$, that is, just outside the Coulomb interference region, the cross section varies quite accurately as $(1/E)$ for E from 40 Mev to 147 Mev, provided the 93-Mev results are increased by the absorber correction of about 15%. For this range of energies the variation of cross section may be represented by a simple power law even for q

as large as 1.25, where it is $(1/E)^{0.62}$. The 206-Mev and 312-Mev cross sections do not conform to a simple power law, consistent with the lower-energy results, at any value of q . However, the variation of cross section with E for constant q is quite systematic as is shown in Fig. 6. Values interpolated from Fig. 4 have been used as the "experimental" points, and a certain amount of imagination has been exercised in drawing the curves. The principal feature of Fig. 6 is the occurrence of a minimum cross section, σ_{min} , at an energy E_{min} for a given q , and the shift of E_{min} to smaller energies with increasing q . It is not clear that these observations have any relevance. (c) For a fair range of q greater than 0.5, the cross sections may be represented by Gaussian functions of the form $\exp(-a^2q^2/2)$. For the 40-Mev to 147-Mev data, $a \sim 1.8$ fermi [$1 \text{ fermi (f)} \equiv 10^{-13} \text{ cm}$], while for 206 and 312 Mev, a must be taken to be significantly less.

The main feature of the variation of polarization with energy is the way in which the maximum value changes. As the energy drops, the first maximum increases from nearly 0.8 at 312 Mev to nearly 1 at 206 Mev and apparently stays at that value down to 147 Mev. Below this energy, it drops rapidly to about 0.1 at 66 Mev. There are no experimental results between 66 Mev and 17 Mev, at which energy there is a measurement by Brockman.¹² However, Gammel and Thaler¹³ have calculated the polarization for energies up to 40 Mev by extrapolating phase shifts found from low-energy cross-section measurements. Their calculations show a continuation of the trend mentioned above, namely a steady drop in the value of the first maximum of polarization with decreasing energy. This leads to a reversal of sign, the first maximum and minimum being replaced by a large minimum and maximum at low energies. Brockman's measurement is in agreement with these calculations at 17 Mev. Hence there is an energy near 40 Mev at which the polarization is almost zero for a large range of angles. For example, at 40 Mev, Gammel and Thaler find

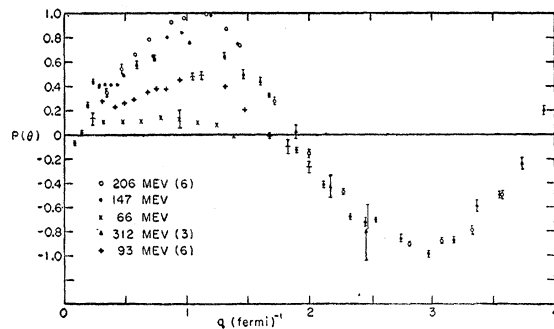


FIG. 5. p - α polarization vs q at several energies. A few typical errors are shown.

¹² K. W. Brockman, Phys. Rev. **108**, 1000 (1957).

¹³ J. L. Gammel and R. M. Thaler, Phys. Rev. **109**, 2041 (1958).

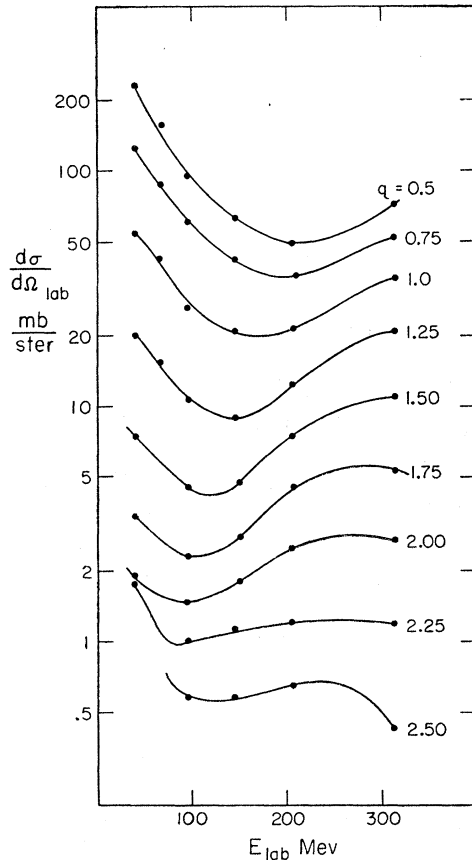


FIG. 6. p - α laboratory differential cross section as a function of energy for fixed values of q . The 93- and 206-Mev data are not corrected for absorption in the counter telescopes.

that the polarization is in the range -0.1 to 0.1 for $0^\circ \leq \theta_{c.m.} \leq 90^\circ$.

In Fig. 7 are plotted smooth curves representing the polarizations measured at energies near 150 Mev for different spin-zero nuclei. Again the momentum transfer has been taken as the abscissa to take energy differences into account. The steady trend of the first maximum and minimum with atomic number is clear. The similarity between the 155-Mev results for carbon and the 147-Mev results for helium within the first peak will be commented on below.

IV. DISCUSSION

It has become conventional¹¹ to describe the nuclear scattering by complex nuclei by a central potential and a Thomas-type spin-orbit potential. We write this in the form

$$(1+i\beta)V_1(r) + \lambda^2 \frac{1}{r} \frac{dV_2(r)}{dr} \mathbf{L} \cdot \mathbf{S}, \quad (1)$$

where λ is the reduced Compton wave length of the proton. The optical-model potentials V_1 and V_2 must be related to the nucleon-nucleon interactions in some

way, and some progress in this direction in a general way has been achieved by Tamor.¹⁴ The work of Bethe¹ and McManus and Thaler² has been more specific, and they have succeeded in relating the cross sections and polarizations observed in scattering from complex nuclei directly to the nucleon-nucleon phase shifts as inferred from experiment at 310 Mev. Before discussing their work in more detail, we make some observations on the relation of V_1 to V_2 within the framework of the optical model.

If $V_2 = \alpha V_1$, then in the first Born approximation the polarization, P , due to the potential (1) may be shown to be¹¹

$$P(\theta) = \frac{\alpha \beta k^2 \sin \theta}{1 + \beta^2 + \frac{1}{4} \alpha^2 k^4 \sin^2 \theta}. \quad (2)$$

As has been pointed out by Malenka¹⁵ and Levintov *et al.*,¹⁶ the expression (2) for P is essentially positive, it has a single maximum, and it is independent of the shape of the potential. Comparison with the polarization data of Figs. 5 and 7 shows that (2) is a very poor approximation to the measured values except perhaps well within the first diffraction minimum, and it does not reproduce any of the large variations of the polarization. For various reasons, the discrepancy cannot be blamed on a failure of the Born approximation. Levintov¹⁷ and Kohler¹⁸ have shown that Eq. (2) is true under conditions much less stringent than the conditions for the validity of the Born approximation. They do not need to assume V_1 small, but only V_2 small if $V_1(r) \propto V_2(r)$.

The Kohler-Levintov theorem breaks down near the diffraction minima and the characteristic feature is a dip in the polarization curve at these points, followed

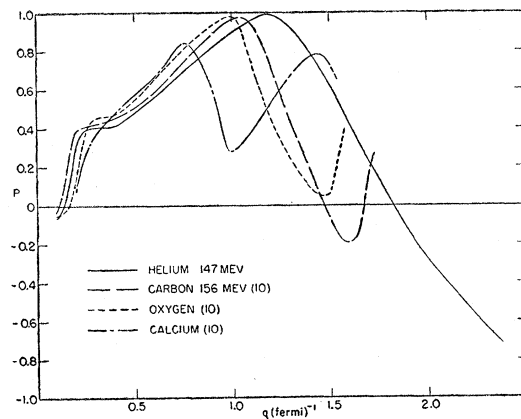


FIG. 7. Measured polarizations in the elastic scattering of protons by various spin-zero nuclei, plotted against q .

¹⁴ S. Tamor, Phys. Rev. **97**, 1077 (1955).

¹⁵ B. J. Malenka, Phys. Rev. **95**, 522 (1954).

¹⁶ Levintov, Miller, and Shamshev, Nuclear Phys. **3**, 221 (1957).

¹⁷ I. I. Levintov, Doklady Akad. Nauk S.S.S.R. **107**, 240 (1956) [translation: Soviet Phys. Doklady **1**, 175 (1956)].

¹⁸ H. S. Kohler, Nuclear Phys. **1**, 433 (1956).

by a rise to the Born approximation curve at larger angles. Exact numerical solutions of the Schrödinger equation have been calculated by Bjorklund *et al.*¹⁹ using Riesenfeld-Watson potentials and again assuming $V_1 \propto V_2$. These reproduce the dips in the polarization for heavy nuclei only moderately, but fail completely for helium at angles of about 60° where the experimental result is close to -1 and the theory is close to $+1$. Lastly, Malenka¹⁵ has shown that substantial negative polarizations may be obtained even in the Born approximation if V_1 and V_2 are not assumed proportional. Hence we conclude, with Levintov *et al.*,¹⁶ that it is very unlikely that the assumption $V_1 \propto V_2$ is true.

This is supported from a different point of view by the aforementioned work of McManus and Thaler,² which extends the work of Bethe.¹ They describe the small-angle scattering from complex nuclei by a Born approximation scattering amplitude $g_B(E, q)$ which they write

$$g_B(E, q) = \bar{M}(E, q) F(q) N. \quad (3)$$

$\bar{M}(E, q)$ is the two-nucleon scattering amplitude, averaged over the spin directions of the target nucleons, and corrected for differences between two-nucleon and nucleon-nucleus scattering kinematics. $F(q)$ is the nuclear form factor, which, since it depends only on the distribution of nucleons in the nucleus, ought not to depend on E , the energy of the incident nucleon. N is the number of nucleons in the target nucleus. For spin-zero nuclei, \bar{M} may be written as the sum of two complex amplitudes

$$\bar{M}(q) = A(q) + C(q)\sigma_n, \quad (4)$$

where σ_n is the component of the spin (of the incident

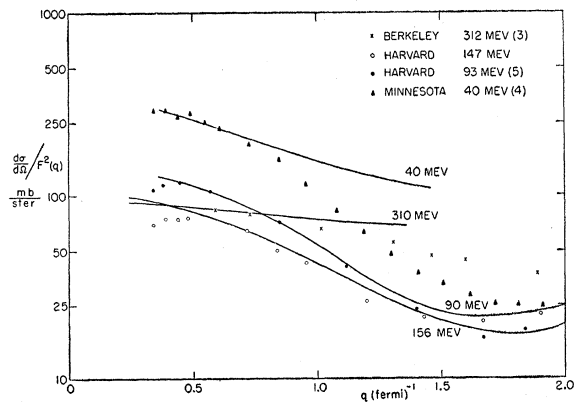


FIG. 8 Comparison of experimental p - α differential cross sections (in the laboratory system) with the KMT²⁰ calculations (solid curves). The theoretical curves have been normalized to the experimental results by multiplying the former by factors of 0.39, 0.42, 0.42, and 0.60, respectively, as the energy increases from 40 to 310 Mev. $F(q)$ is the form factor.

¹⁹ Bjorklund, Blandford, and Fernbach, *Phys. Rev.* **108**, 795 (1957).

proton) perpendicular to the plane of scattering. In their analysis, McManus and Thaler derive four mean-square radii $\langle a^2 \rangle_n$, $n=1, 2, 3, 4$. The first two arise from the spin-independent amplitude and the second two from the spin-dependent amplitude. In their calculations for carbon, they assumed that $F(q)$ was derived from the charge distribution as determined by electron scattering, and they found that the averages of the two pairs, which give radii of V_1 and V_2 , respectively, in a rough way, were indeed different and varied quite considerably with energy. This adds considerable support to the conclusion that V_1 is not proportional to V_2 .

The work of McManus and Thaler has been extended by Kerman, McManus, and Thaler,²⁰ hereafter referred to as KMT. With the expression (4) for \bar{M} , they write

$$(d\sigma/d\Omega)_{\text{lab}} = (2N)^2 [|A|^2 + |C|^2] F^2(q), \quad (5)$$

$$P = 2 \text{Re}(A^*C) / (|A|^2 + |C|^2), \quad (6)$$

where A and C are calculated from the two-nucleon phase shifts derived from the Gammel and Thaler potential.²¹

A comparison of experimental results with the KMT calculations is made in Figs. 8 and 9. In the former, the KMT results are represented by $(2N)^2 [|A|^2 + |C|^2]$, normalized to experiment at $q \sim 0.5$, plotted as functions of q for various energies. The experimental results are represented by the measured cross sections divided by $F^2(q)$. The form factor has been found from the Stanford results,²² which show that at both 185 Mev and 400 Mev, electron scattering may be represented by a Gaussian form factor with a mean square radius of 2.59 f^2 . This value for the mean square radius should not be used for $F(q)$ in Eq. (5), since it includes the proton charge distribution, which has a mean square radius of 0.64 f^2 . The proper value for $F(q)$ is the mean square radius of the distribution of nucleon centers, which is found from the Stanford results by subtraction and is 1.95 f^2 . A Gaussian function with this mean square radius has been used for $F(q)$ in calculating the experimental points of Fig. 8. This ignores the effect of multiple scattering. The effect of the multiple-scattering correction will be to increase the experimental values; for small angles and light elements, this increase will be by a constant though not very well determined factor. This can be seen, for example, by an explicit calculation on the optical model. Even a radius derived from an extreme case of an opaque disk is only 12% different from that derived from the optical model.

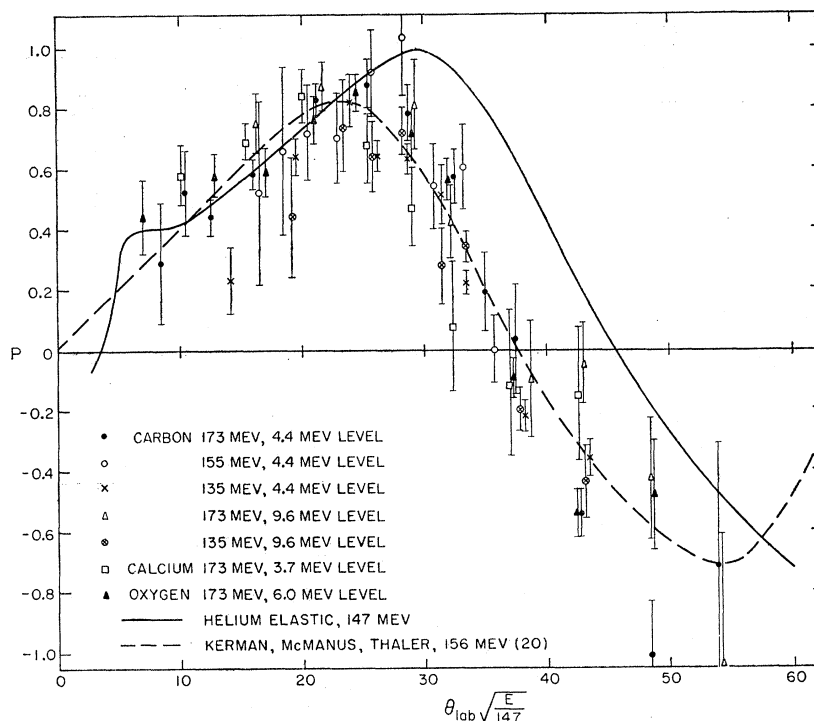
If the nucleon-nucleon scattering amplitudes were constant with angle, the theoretical curves in Fig. 8 would be horizontal straight lines. We have clear evidence of the necessity of introducing this variation and its qualitative change with energy. The quantita-

²⁰ Kerman, McManus, and Thaler (private communication).

²¹ J. L. Gammel and R. M. Thaler, *Phys. Rev.* **107**, 1337 (1957).

²² R. Hofstadter, *Annual Review of Nuclear Science* (Annual Reviews Inc., Palo Alto, 1957), Vol. 7, p. 231.

FIG. 9. Polarizations from inelastic scattering from several elements,²⁶ compared with the p - α elastic scattering at 147 Mev in this experiment and with the theoretically predicted p - α polarization at 156 Mev.²⁰ Energy differences are taken into account by plotting P vs $\theta_{\text{lab}} \times (E/147)^{1/2}$.



tive agreement is bad. At 93 Mev and 147 Mev there is evidence of the constant ratio between the KMT calculations and experiment, which is to be expected from the multiple-scattering correction. What is most surprising is the disagreement at 312 Mev, since the experimental results figure so largely in the determination of the constants of the Gammel and Thaler potential, and hence of their phase shifts.

The agreement between experiment and the KMT calculations of the polarization (shown in Fig. 9) is encouraging. It is far better than would be obtained from a potential of the form (1), with $V_2 = \alpha V_1$, by a Born approximation or even a partial-wave calculation with a high-energy approximation to the phase-shifts. In common with other calculations, those of KMT fail to give a value of very nearly one for the first maximum, but they do not fail as conspicuously. They reproduce the trend towards the first minimum with considerable success. It should be noted [Eq. (6)] that P is independent of the form factor; thus the agreement between theory and experiment is a measure of the accuracy of the calculation of \bar{M} and its angular dependence from the nucleon-nucleon phase shifts.

Calculations of a similar nature to those of KMT have been made by Singh²³ and provide roughly the same agreement with experiment as those of KMT. Recent calculations by Cromer,²⁴ which extend the work of Bethe¹ by using better approximations, have been able to reproduce the polarization of +1 measured in the forward direction.

The polarization data at 66 Mev show agreement with the polarization at small angles from carbon²⁵ at this energy, and with the KMT calculations. This suggests that multiple-scattering corrections still do not affect the polarization at 66 Mev. The high polarization in p - α scattering at a few Mev¹³ is a different phenomenon, where multiple off-energy-shell scattering is dominant; the transition appears to occur about 40 Mev, and here there is no polarization at small angles. These general features therefore suggest that the search for an analyzer in the small-angle region at this energy is hopeless. The large-angle region is not very useful because of the low cross section.

Figure 9 shows the polarizations measured in inelastic scattering from a number of levels in different elements, together with smooth curves representing our 147-Mev elastic p - α measurements and the theoretical p - α curve of KMT. The inelastic data have been taken from Hillman, Johansson, and Tyren.²⁶ KMT have shown that for inelastic scattering, where spin flip is unimportant, the polarization should be the same as that for elastic scattering for angles such that the form factor is unimportant (i.e., unity). Maris²⁷ had already shown this for the special case of collective nuclear excitation.

The cross section at backward angles falls off as $1/E^7$. This is known as the "pickup" region of a triton. The extreme dependence on energy is in accordance with a rapid fall in the momentum distribution of these

²³ J. Dickson (private communication).

²⁶ Hillman, Johansson, and Tyren, *Nuclear Phys.* **4**, 648 (1957).

²⁷ Th. A. J. Maris, *Nuclear Phys.* **3**, 213 (1957).

²³ L. S. Singh (private communication).

²⁴ A. Cromer (private communication).

tritons. The polarization of the pickup alpha is positive (opposite to that of the proton), and the curve convex to the angle axis. This same behavior is noticed in the study of pickup deuterons from carbon²⁸ and in the study of neutron production from complex nuclei by protons.²⁹

A more exact analysis will be made at a later date, by which time we hope to have completed some triple-scattering measurements, which will determine the relative phases of the spin-dependent and spin-independent scattering amplitudes.

²⁸ P. F. Cooper, thesis, Harvard University, 1958 (unpublished).

²⁹ S. G. Carpenter and R. Wilson, Phys. Rev. **113**, 650 (1959).

ACKNOWLEDGMENTS

Many persons have assisted with the experiment in one way or another. In particular we would like to thank Professor S. Collins of the Massachusetts Institute of Technology who readily supplied us with liquid helium when we were in need, and D. Lynch, J. Musher, J. Sanderson, R. Spector, and D. Steinberg, who assisted in taking data and computing. One of us (A.M.C.) wishes to acknowledge the award of an Overseas Bursary by the South African Council for Scientific and Industrial Research, and the hospitality of the Harvard Cyclotron group.

Angular Correlation Measurements in $O^{15}\dagger$

B. POVH* AND D. F. HEBBARD

Kellogg Radiation Laboratory, California Institute of Technology, Pasadena, California

(Received March 2, 1959)

An accurate measurement of the energy of a gamma transition from the 7.56-Mev level in O^{15} discloses that the transition takes place to the 5.19-Mev level in O^{15} rather than to the 5.25-Mev level. Another transition takes place through the 6.15-Mev level. The third known transition occurs through the 6.79-Mev level rather than through the 6.86-Mev level. The angular correlations of cascades from the 7.56-Mev level through the levels at 6.79 Mev, 6.15 Mev, and 5.19 Mev are measured. These results, combined with previous results on these levels, are consistent only with $J^\pi = \frac{3}{2}^+$ and $\frac{3}{2}^-$, respectively, for the 6.79-Mev and 6.15-Mev levels. For the 5.19-Mev level, the present results indicate $J = \frac{3}{2}$, but are consistent also with $J = \frac{5}{2}$, if a suitable mixing ratio of $E2$ to $M1$ radiation is chosen. The preferred assignments are all consistent with the shell-model predictions and with comparisons with the N^{15} level scheme. It is noted that the doublets near 5.2 Mev in O^{15} and N^{15} are reversed in order.

INTRODUCTION

THE recent discovery of the 5.19-Mev and 5.25-Mev states in O^{15} , by means of the $O^{16}(\text{He}^3, \alpha)O^{15}$ reaction,¹⁻³ has opened the question of whether the observed γ transitions from higher levels in O^{15} occur to one or both of these states. The 7.56-Mev level is known to emit gamma rays^{4,5} of energy 2.4 ± 0.1 Mev as well as gamma rays of energies 1.39 and 0.77 Mev, with relative intensities in the ratio 2:8:3. This level occurs as a resonance in the reaction $N^{14}(p, \gamma)$ at 277 kev.¹ The expected energies of the transitions to the 5.2-Mev doublet are 2.31 and 2.37 Mev. Because of this appreciable difference in gamma energies, an experiment was planned to measure accurately the transition energy. The 7.56-Mev level is known to be $\frac{1}{2}^+$ from

proton elastic scattering measurements,^{1,4} and the known isotropic gamma-ray distributions.^{4,6} The doublet, on shell-model considerations,⁷ is expected to be $\frac{1}{2}^+$ and $\frac{5}{2}^+$. These spin assignments would favor the $\frac{1}{2}^+ \rightarrow \frac{1}{2}^+$ transition, rather than the $\frac{1}{2}^- \rightarrow \frac{5}{2}^+$ transition, leading to the hope that only one member of the 5.2-Mev doublet would be involved in the cascade.

Information on the spin of the intermediate state can be obtained by angular correlation measurements. Measurements have already been made by Gorodetzky *et al.*⁸ on transitions from the 8.28-Mev $\frac{3}{2}^+$ level to the 5.2-Mev doublet. Unfortunately, no distinction could be made between the members of the doublet, both of which should act as intermediate states. The measured

[†] Supported in part by the joint program of the Office of Naval Research and the U. S. Atomic Energy Commission.

* On leave from The "J. Stefan" Institute, Ljubljana, Yugoslavia.

¹ F. Ajzenberg-Selove and T. Lauritsen, Nuclear Phys. (to be published).

² Allen, Middleton, and Hinds (private communication).

³ B. Povh, Phys. Rev. **114**, 1114 (1959).

⁴ R. E. Pixley, Ph.D. thesis, California Institute of Technology, 1957 (unpublished).

⁵ Johnson, Robinson, and Moak, Phys. Rev. **85**, 931 (1952).

⁶ The angular distributions of the three low-energy gamma rays have been recently remeasured at the Kellogg Radiation Laboratory, and are found to be isotropic within 2%. The high-energy gamma-ray distributions are also consistent with isotropy. S. Bashkin (private communication) reports that his latest results are also in agreement with isotropy, superseding the earlier report of anisotropy [Bashkin, Carlson, and Nelson, Phys. Rev. **99**, 107 (1955)].

⁷ E. Halbert and J. B. French, Phys. Rev. **105**, 1563 (1957).

⁸ Gorodetzky, Gallmann, Croissiaux, and Armbruster, Nuclear Phys. **6**, 517 (1958).